Wei Li[1], Weidong Shi[1], Xiaoping Jiang[1], Ting Jiang[1], Bin Chen[1]

Research Center of Fluid Machinery Engineering and technology, Jiangsu University, P. R. China (1)

Impact of the Volute Basic Circle Diameter of Sewage Pump on Pressure Pulsation

Abstract. *The unsteady flow field in the channel sewage pump with three different basic circle diameters of volutes were numerically simulated based on the Fluent commercial software, using the standard k-ε turbulence model, the SIMPLE algorithm, and the sliding mesh technique. By setting pressure measurement points, the pressure pulsation in different positions can be obtained. The impact of the basic circle diameter of volute on the internal pressure pulsation characteristics of a sewage pump was analyzed based on frequency domain and time domain graphs. The results show that the smaller the basic circle diameter of volute is, the more turbulent the pressure pulsation is. The Coefficient of pressure pulsation amplitude reaches the maximum value with small gaps in the volute and impeller clearance. The closer the monitoring point to the cutwater, the greater the amplitude of pressure pulsation. In a flow channel of volute, the pressure fluctuation presents cyclical changes, and a small gap flow reaches the strongest unsteady characteristics. Pressure pulsation cycle is associated with the number of impeller blades and a period of three peaks is the blade passing frequency. The dominant frequency of pressure pulsation is 73.5Hz, which is the threefold frequency of rotation frequency.*

Streszczenie. *W artykule przedstawiono wyniki i opis symulacji przepływu w pompie kanalizacyjnej z trzema różnymi średnicami sprężyn napędowych. W badaniach wykorzystano oprogramowanie Fluent, jeden ze standardowych modeli turbulencji (k-epsilon), algorytm SIMPLE oraz technikę siatki przesuwnej. W analizie skupiono się na przypadku wystąpienia zakłóceń przepływu w kanale. Dokonano analizy wyników i przedstawiono wnioski. (**Pulsacje ciśnienia w pompie kanalizacyjnej – wpływ średnicy śruby napędowej**).*

Keywords: Sewage pump, Volute, Basic circle diameter, Unsteady flow, Pressure pulsation.
Słowa kluczowe: pompa kanalizacyjna, średnica koła bazowego, niestabilny przepływ, pulsacje ciśnienia.

1. Introduction

Submersible sewage pumps are sewage discharge equipment as two in one of the motor and pump, which have a wide range of applications in the field of flood control and drainage, and urban sewage discharge. In order to improve the drainage capacity of the sewage pump and realize non-overload characteristics, this paper designed high efficient non-overload channel submersible sewage pump[1]. The performance of the pump is determined both by impeller and volute, but it has long been that the research focus primarily on the impact of throat area on the pump performance, and has ignored the performance degradation and destruction due to mismatch impeller and volute[2]-[4]. Preliminary studies found that, to control flow and reduce flow space, under conditions of extreme thickening blades, due to water outflow from impeller only part of the area on the circumference of impeller outlet, so the flow is unevenly distributed, and is bound to deteriorate the flowing condition within volute. Meanwhile because of the characteristics of three-dimensional non-axial symmetry of the volute shape, the interaction between the dynamic and static components of impeller and volute makes the internal flow field produce complex non-stability[5]-[7]. The generation of pressure pulsation within internal flow field affects the efficiency and stability of the pump, along with flow separation, cavitation, and triggering the instability of the vibration and noise[8]-[11].

In this paper, through numerical calculation of three-dimensional unsteady flow for three different basic circle diameters of volute, pressure pulsation at monitoring point is obtained, and through the analysis of time domain and frequency domain of pressure pulsation, the impact pattern of basic circle diameter of volute on the pump exterior characteristic and pressure pulsation is mastered, which provides a theoretical basis to improve the performance and stability of the channel submersible sewage pump.

2. Numerical Simulation Methods

2.1. Physical mode

In order to improve the sewage capacity of the pump, this paper uses thickening blade design, and the main design parameters are: flow Q=150m^3/h, Head H=48m, speed n=1470r/min, Rated supporting power P=45kW. The model geometry parameters: the three-channel impeller thicker leaves, leaf number z=3, the impeller diameter D_2=385mm, outlet width b_2=40mm, blade wrap angle φ =225°, blade outlet angle β_2 =14°. Approved the maximum particle diameter is 30mm.

Selected three cases with different basic circle diameters of volutes are as follows: case 1: D_3=390mm, case 2: D_3=435mm, and case 3: D_3=460mm. Volute inlet width b_3 = 60mm.

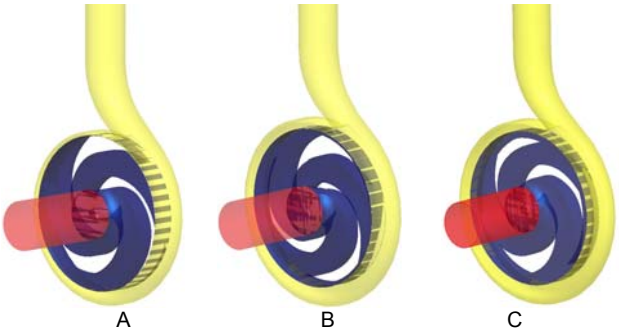

Fig.1. Calculation model：(A) D_3=390mm (B) D_3=435 mm (C) D_3=460mm.

2.2. Calculation model and mesh generation

The computational domain is the entire flow path from the impeller inlet to volute outlet as shown in Fig. 1. Three-dimensional solid model of pump is processed with Pro/E software, and the three-dimensional stereogram is generated in accordance with the two-dimensional hydraulic diagram. The mesh generation is realized with Fluent's preprocessing software Gambit, and the overall division of mesh is processed with strong adaptability Tgrid mixed grid. When the number of grid reaches 2 million, a maximum difference of the efficiency of the pump is up to 0.5%, and is toward stabilization. Taking into account the coordination of computing time and accuracy and the similar sizes in each group case, the total number of more than 1.5 million grids will meet the computational accuracy requirements.

2.3. Control equation

According to the mass and momentum conservation, the standard model *k-ε* is used, the transport equation with turbulent kinetic energy *k* and turbulent kinetic energy dissipation rate *ε* is as follow:

(1) $$\mu_t = \rho C_\mu \frac{k^2}{\varepsilon}$$

(2) $$\frac{\partial(\rho k)}{\partial t} + \frac{\partial(\rho k u_i)}{\partial x_i} = \frac{\partial}{\partial x_j}\left[\left(\mu + \frac{\mu_t}{\sigma_k}\right)\frac{\partial \varepsilon}{\partial x_j}\right] + G_k - \rho\varepsilon$$

(3) $$\frac{\partial(\rho \varepsilon)}{\partial t} + \frac{\partial(\rho \varepsilon u_i)}{\partial x_i} = \frac{\partial}{\partial x_j}\left[\left(\mu_\varepsilon + \frac{\mu}{\sigma_\varepsilon}\right)\frac{\partial \varepsilon}{\partial x_j}\right] + \frac{C_{1\varepsilon}}{k} G_k - C_{2\varepsilon}\frac{\rho \varepsilon^2}{k}$$

where μ_t is the turbulent viscosity, C_μ, $C_{1\varepsilon}$ and $C_{2\varepsilon}$ are the empirical constants, G_k is the turbulent kinetic energy *k* generated by mean velocity gradient, σ_k and σ_ε are the Prandtl numbers corresponding to turbulent kinetic energy *k* and dissipation rateε *ε*, respectively. Model constant values are as follows: C_μ=0.09, $C_{1\varepsilon}$=1.44, $C_{2\varepsilon}$=1.92, σ_k=1.0, σ_ε=1.3.

2.4. Boundary conditions

Based on Fluent, the SIMPLE method is used to solve the incompressible mean time *N-S* equations. The standard *k* -ε model is selected as turbulence model. The Channel wall surface is with no-slip boundary conditions. The near channel wall surface area is treated with the standard wall function treatment. The speed inlet boundary condition is used for inlet, and the free flow boundary condition is used for outlet.

Through the grid-independent analysis, unsteady numerical calculation is processed based on convergence of three-dimensional steady turbulent flow. At every 3° of the impeller rotation, one time step turbulence converged solution is obtained. The converged solutions on all time steps constitute a non-steady solution, namely, the process of change of pressure and speed over time in entire flow channel, which gives the pressure pulsation in the flow field. The time-step calculation is determined by the speed of the selected pump. When the speed is 1470r/min, and Δt = 0.000340136s, a 120 steps impeller can rotate a whole circle. After three computation cycles, the numerical experiments found that the velocity field and pressure field changes produced by non-steady calculation meets periodic requirements, and the calculation converges. This paper selects the design conditions of the sewage pump for this study.

Pressure pulsation monitoring points were set in the volute flow channel and the clearance between volute and impeller as shown in Fig. 2A, where p_i (*i*= 1,2 ... 8) is monitoring point within volute flow channel, p_j (*j*= 1,2 ... 8) is monitoring point at the clearance between impeller and volute. Fig. 2 shows that eight monitoring sites are selected as representative points for the analysis of pressure pulsation, in which points of P_1, P_2, P_3, and P_4 are at the same radius of the clearance between volute and impeller, points of P_5, P_6, P_7, and P_8 are located in the volute flow channel, and its position distribution is shown in Fig. 2B.

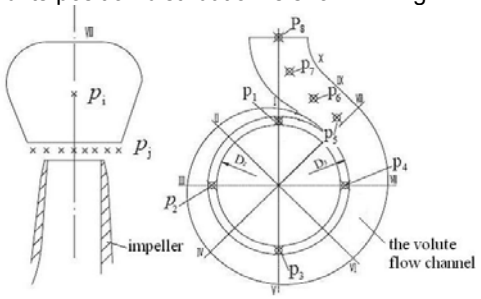

A B

Fig. 2. Location diagram of pressure monitoring points.

3. Experiment Verification

3.1. Experimental device

To verify the accuracy of the numerical calculation, an open centrifugal pump performance test rig is built as shown in Fig.3. The test rig meets grade 1 accuracy requirements. The test site and installation are shown in Fig. 3.

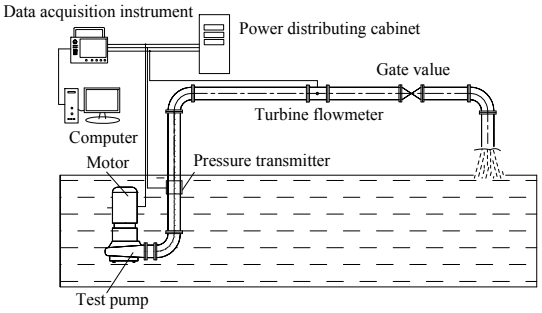

Fig. 3. Diagram of the test device and test site.

3.2. Test result and analysis

Take case 2 as an example, three curves are developed by measuring the flow-head curve, flow-efficiency curve, and flow-power curve, respectively, and the external characteristic curve is drawn for sewage pump test and unsteady numerical calculation as shown in Fig. 4.

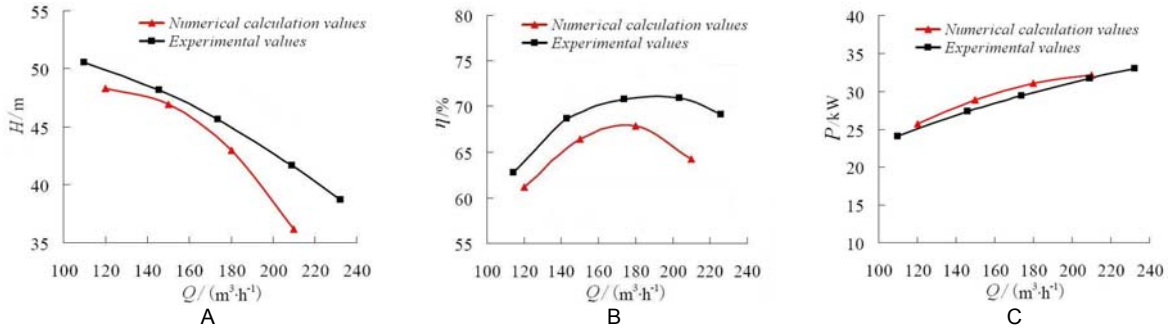

A B C

Fig. 4. Comparison of external characteristics predicted curve and test curve: (A) flow-head curve (B) flow-efficiency curve (C) flow-power curve.

The analysis on above diagram shows that the external characteristics curve calculated by the numerical calculation agrees well with test results. The relative error of the efficiency, the head, and the shaft power were 4.22%, 4.35% and 6.89%, respectively, at maximum efficiency points of numerical calculation results and test results. The head and efficiency curves predicted by unsteady numerical calculation tend to be low while the power prediction curve is relatively high. The main reason may be due to the loss calculations are determined by relying on the empirical formula, whereas there are errors in the empirical formula. For example, the quantity of leakage is closely associated with disk friction losses, but this paper only considers its relationship with the specific-speed. According to the analysis of test results and unsteady numerical calculation results, using the grid type, the turbulence model, etc. can more accurately predict the external characteristics of sewage pump.

4. Analysis of Pressure Pulsation

4.1.Time-domain analysis of pressure pulsation

The time domain diagram of the pressure pulsation of monitoring points in clearance area between volute and impeller within a cycle as shown in Fig. 5. As can be seen from diagram, the pressure monitoring points with all cases display cyclical variation pattern. However, the pressure pulsation of cases 2 and 3 showed significant sine wave-like cyclical, whereas the pressure pulsation of case 1 is slightly disordered. The amplitude of pressure pulsation coefficient for case 1 is the largest and is three times bigger than the other cases. The pressure pulsation trend at each monitoring point in the case 2 and 3 is almost the same, and they completely overlap at the P3 point. The order of amplitude value is: case 1>case 2>case 3. This means that under design condition, dynamic static coupling of the impeller and volute is the reason causing the pressure pulsation. The smaller the basic circle diameter of volute is, the more intense the pressure pulsation is. However, when the basic circle diameter increases from 435mm to 460mm, the dynamic static coupling has less influence to static pressure at each monitoring point in the clearance between volute and impeller. Three peaks appear in an impeller rotation period, which is consistent with the number of impeller blades, that is, the pressure pulsation period is T = 120°. The closer the monitoring point from cutwater, the bigger the amplitude of the pressure pulsation coefficient. The overall fluctuation amplitude trend are: P1> P2> P3> P4, that means the gradual decay of the pressure pulsation along the direction of impeller rotation.

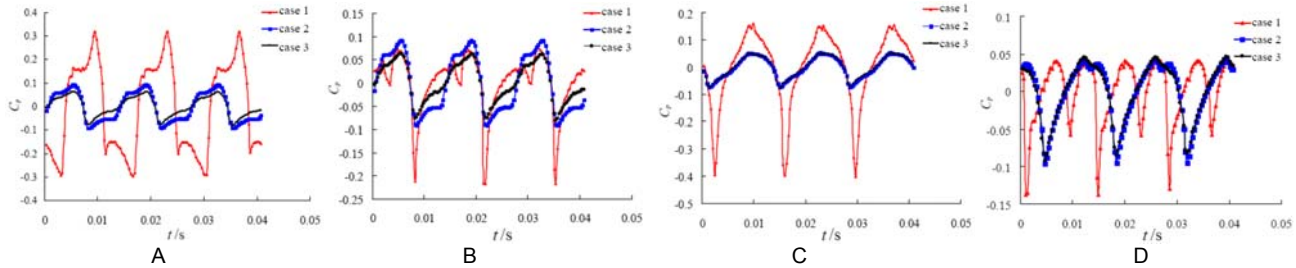

Fig. 5. Time-domain diagram of the pressure pulsation at (A) P1 point, (B) P2 point, (C) P3 point and (D) P4 point in clearance between volute and impeller.

The time domain diagram of the pressure pulsation of monitoring points in volute flow channel within a cycle as shown in Fig. 6. As can be seen from diagram, under the design condition, the pressure pulsation of each monitoring point within the volute flow channel appears cyclical changes in a period, and shows three peaks in a period, which is the blade passing frequency. The case 1 has the largest amplitude of pressure pulsation coefficient, and the strongest unsteady characteristic in volute flow channel, as well as the relatively disordered pressure pulsation. The pressure amplitude is almost the same at points P6, P7, and P8 and is greater than the amplitude of pressure pulsation coefficient at point P5. The pressure pulsation trend is almost exactly the same for case 2 and case 3 in a sine wave form. The pressure amplitude at points P6, P7, and P8 is basically the same, and is three times bigger than one at point P5. That means that the pressure pulsation signal comes from the volute outlet. The order of amplitude value is: case 1> case 2> case 3.

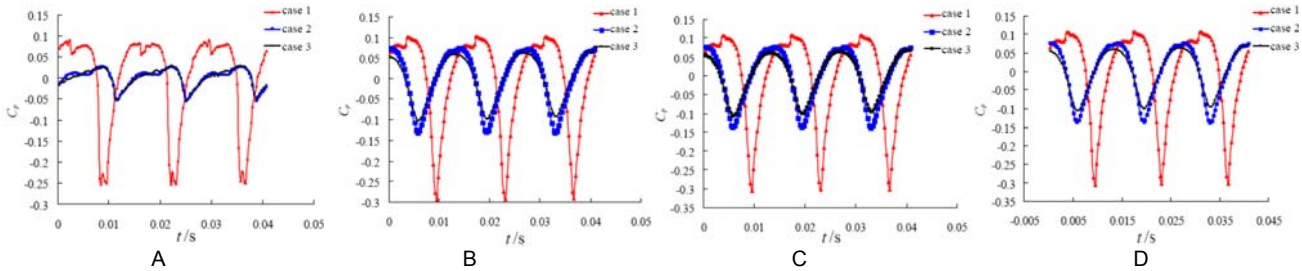

Fig. 6. Time-domain diagram of the pressure pulsation at (A) P5 point, (B) P6 point, (C) P7 point and (D) P8 point in volute flow channel.

4.2. Frequency domain analysis of pressure pulsation

The frequency domain diagram produced by Fast Fourier Transform (FFT) for different cases, as in Fig. 7, is consistent with the analysis results of pressure pulsation. Because of the smaller clearance between volute and impeller for case 1, its amplitude of the pressure coefficient is significantly higher than other cases. The blade frequency for case 1 is three times bigger than other cases, while the amplitude and pulsation frequency for case 2 and case 3 are relatively closer each other. The altitude of pressure pulsation for case 1 at point P1 near cutwater is clearly larger than one at other location. The impeller speed in this article is n=1470r/min, then rotation frequency is 24.5Hz, the number of impeller blades is z=3, the blade passing frequency (BPF) is 73.5Hz. In the fluid pressure pulsation, the impact frequency of the impeller blades on the fluid is

equal to z times of rotation frequency and harmonic. It can be seen from the frequency domain graph of pressure pulsation that the pressure pulsation main frequency is 73.5Hz, that is, rotation frequency tripling.

When integrating the time domain analysis and frequency domain analysis of pressure pulsation at the monitoring points for various cases, because of the thicker outlet of extra-thick blade, the different basic circle diameters have a great impact on internal flow of pump. The smaller basic circle diameter results in the very small gap between impeller and volute, non-conducive to the impeller outlet fluid mixing and volute pressure diffusing, increasing pump flow turbulence, and affecting the performance and stability of the pump operation. If the basic circle diameter is too large, although it doesn't affect the pressure pulsation too much, but it would reduce the pump efficiency. Therefore, case 2 can be selected as preferred case because its base circle size is reasonable and the volute pressure diffusing performance is better.

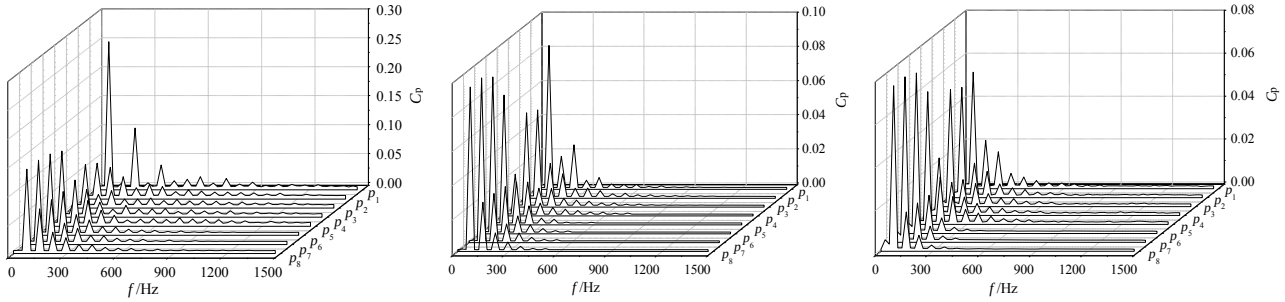

Fig. 7. Frequency domain diagram of monitoring point for different cases

5. Conclusions

The basic circle diameter of volute has greater impact on pressure pulsation of whole flow field of channel submersible sewage pump. In the volute and impeller clearance, the smaller the basic circle diameter and the smaller the gap between the impeller and the volute, the greater the amplitude of the pressure coefficient is. The blade frequency amplitude in case of small clearance is three times bigger than the one over other cases. Especially the pressure pulsation amplitude near cutwater is much bigger than the one in other locations. Inside volute flow channel, the pressure pulsation changes in cyclic, and it is also the case that the non-steady characteristics of small gap flow becomes the strongest and the pulsation is more disordered. The pressure pulsation cycle is associated with the number of impeller blades, and the pulsation main frequency is the threefold rotation frequency.

In consideration of the sewage capacity, increasing the width of the impeller outlet and significantly increasing the blade thickness can block a portion of flow channel, thereby reduce the impeller outlet area and control flow. Because the control capacity of three-blade structure impeller on the liquid weakened, the wake region becomes bigger, and the heterogeneity of the impeller outlet flow field is greater than the general centrifugal pump. Therefore, in the design of channel submersible sewage pump, increasing the basic circle diameter is conducive to uniform flow in the volute, thereby enhance the efficiency of the pump and flow stability.

Acknowledgments

This work was sponsored by the Natural Science Foundation Project of Jiangsu Province (No.BK2011505), PAPD, the Scientific and Technological Innovation team Project of College in Jiangsu Province (No.[2009]10), the Natural Science Foundation Project of College in Jiangsu Province (No.09KJD570001), the Graduate Innovation Project of Jiangsu Province (No.CX09B_196Z).

REFERENCES

[1] Shi Weidong, Jiang Ting, Cao Weidong., Optimal design and experiment on a high-head non-overload submersible sewage pump. Transactions of the CSAE, 2011, 27(5): 151-155.

[2] H Wang，H Tsukamoto., Fundamental analysis on rotor-stator interaction in a diffuser pump by vortex method. ASME, J.of Fluid Eng, 2001, 123：737-747.

[3] Guo Pengcheng, Luo Xingqi, Liu Shengzhu., Numerical simulation of 3D turbulent flow fields through a centrifugal pump including impeller and volute casing. Transactions of The Chinese Society of Agricultural Engineering, 2005, 21(8)：1-5.

[4] Young- Do Choi, Junichi Kurokawa, Jun Matsui., Performance and internal flow characteristics of a very low specific speed centrifugal pump. Journal of Fluids Engineering , 2006,128: 341-349.

[5] Longatte F, Kueny J L., Analysis of rotor-stator-circuit interactions in a centrifugal pump. Proceedings of the 3rd ASME/JSME Joint Fluids Engineering Conference, 2009:1039－1045.

[6] Barrio R, Parrondo J, Blanco E., Numerical analysis of the unsteady flow in the near-tongue region in a volute-type centrifugal pump for different operating points. Computers & Fluids, 2010, 39: 859－870.

[7] Brennen C E，Acosta A J., Fluid-induced rotordynamic forces and instabilities. Structural Control and Health Monitoring，2006，13(1)：10-26.

[8] Jose Gonzalez，Carlos Santolaria., Unsteady flow structure and global variables in a centrifugal pump. ASME，J. of Fluid Eng，2006，128：937-946.

[9] José González，Joaqun Fernández，Eduardo Blanco., Numerical Simulation of the Dynamic Effects Due to Impeller-Volute Interaction in a Centrifugal Pump. Transactions of the ASME，2002，124(7) : 348-354.

[10]Karassik IJ., Pump Handbook. McGraw-HILL BOOK COMPANY, 1976.

[11]Kitano Majidi., Numerical study of unsteady flow in a centrifugal pump. ASME Journal of Turbomachinery，2005，127(2) : 363-371.

Authors: *Wei Li, Weidong Shi, Xiaoping Jiang, Ting Jiang and Bin Chen. Research Center of Fluid Machinery Engineering and technology, Jiangsu University, Zhenjiang 212013, P. R. China.*